JACS
JOURNAL OF THE AMERICAN CHEMICAL SOCIETY
Article
pubs.acs.org/JACS

Photostability Can Be Significantly Modulated by Molecular Packing in Glasses

Yue Qiu,[†] Lucas W. Antony,[‡] Juan J. de Pablo,[‡] and M. D. Ediger*[,†]

[†]Department of Chemistry, University of Wisconsin—Madison, Madison, Wisconsin 53706, United States
[‡]Institute for Molecular Engineering, University of Chicago, Chicago, Illinois 60637, United States

Supporting Information

ABSTRACT: While previous work has demonstrated that molecular packing in organic crystals can strongly influence photochemical stability, efforts to tune photostability in amorphous materials have shown much smaller effects. Here we show that physical vapor deposition can substantially improve the photostability of organic glasses. Disperse Orange 37 (DO37), an azobenzene derivative, is studied as a model system. Photostability is assessed through changes in the density and molecular orientation of glassy thin films during light irradiation. By optimizing the substrate temperature used for deposition, we can increase photostability by a factor of 50 relative to the liquid-cooled glass. Photostability correlates with glass density, with density increases of up to 1.3%. Coarse-grained molecular simulations, which mimic glass preparation and the photoisomerization reaction, also indicate that glasses with higher density have substantially increased photostability. These results provide insights that may assist in the design of organic photovoltaics and light-emission devices with longer lifetimes.

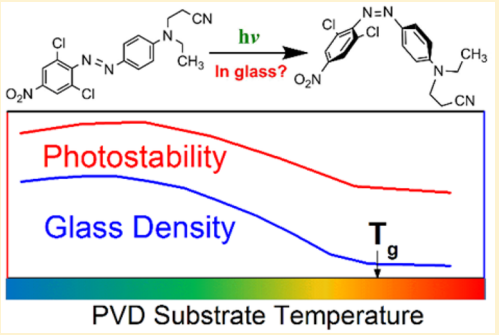

1. INTRODUCTION

Glasses are amorphous materials that have wide usage in modern technology, including polymers,[1] pharmaceuticals,[2] solar cells,[3] and organic electronics.[4,5] For many applications, organic materials prepared as amorphous states are preferred over crystalline solids. For example, in the pharmaceutical industry, some drugs are formulated as glasses due to their higher solubility and bioavailability.[6,7] In the organic electronics field, glasses are frequently used in device fabrication to provide smooth and homogeneous layers.[4] One important issue for organic glasses is photochemical stability. Photodegradation can cause the failure of organic electronics in both display and light-harvesting technologies, and this is sometimes a more limiting factor than device efficiency.[8,9] Photodegradation can be caused by light in the environment or by self-emission,[9,10] so photochemically robust materials are in demand.[10,11]

Previous work has shown that modification of local packing in glasses has a negligible effect on photostability in comparison to what has been observed for crystalline materials. Organic molecules can have very different photoreactivities in different crystal polymorphs. In the pioneering work in topochemistry, Schmidt et al. studied the [2 + 2] photodimerization of cinnamic acid in the solid state. This compound crystallizes in three polymorphic forms which exhibit different photochemical reactivity upon irradiation.[12] An even more striking example is provided by tetrabenzoylethylene, which can undergo unimolecular photoisomerization. Of the two crystalline modifications, one polymorph is light-stable, while the other photoisomerizes to the furanone.[13] In contrast, for amorphous materials, it has been found that photoreactivity depends only slightly on the manner in which the glass is prepared. Torkelson et al. reported that for 4,4′-diphenyl azobenzene dispersed in amorphous polycarbonate the susceptibility to photoisomerization decreased by about 5% after physical aging for 100 h; aging generally increases the density of a glass.[14] We are not aware of a literature precedent showing significant tuning of photoreactivity in organic glasses through control of local packing.

Recently, physical vapor deposition (PVD) has been used to prepare glasses with exceptional properties that are not accessible by any other preparation method.[15−20] By properly controlling processing conditions such as deposition rate and substrate temperature, vapor deposition can form stable glasses that have higher density and enhanced kinetic stability relative to that of traditional liquid-cooled glasses. Typically, the optimal substrate temperature for preparing these PVD glasses is about $0.85T_g$, where T_g is the glass transition temperature. Vapor-deposited glasses can exhibit enhanced kinetic stability; upon heating at a constant rate, a stable glass can maintain its glassy packing to a much higher temperature than a liquid-cooled glass. Vapor-deposited glasses also have densities up to 1.4% higher than that of the corresponding liquid-cooled glass.[21] It has been estimated that a liquid-cooled glass would have to be physically aged for thousands to millions of years to achieve a glass with the same density.[22] Many of the features observed in experimental PVD glasses, including high density and high kinetic stability, have also been observed in computer simulations that mimic the vapor deposition process.[20,23,24]

Received: June 20, 2016
Published: August 12, 2016

DOI: 10.1021/jacs.6b06372
J. Am. Chem. Soc. 2016, 138, 11282−11289

In this work, we test whether the extraordinary kinetic stability and high density of PVD glasses also lead to extraordinary photostability. As a model system, we investigate the photostability of vapor-deposited and liquid-cooled glasses of 3-[[4-(2,6-dichloro-4-nitrophenyl)azo]-*N*-ethylanilino]-propionitrile (also known as Disperse Orange 37 or DO37), an azobenzene derivative. Azobenzenes can undergo trans → cis photoisomerization reactions when irradiated by light; the cis state will relax back to the trans state spontaneously because the trans state is thermodynamically more stable. We vapor-deposited DO37 onto substrates held at different temperatures and successfully obtained glasses with different initial densities and a wide range of kinetic stabilities. Using spectroscopic ellipsometry, the photostability of the different DO37 glasses during light irradiation was characterized by changes in the glass density and birefringence. In this way, the photostability of a series of glasses with identical composition but different densities could be easily compared.

We find that photostability of vapor-deposited DO37 glasses can be significantly modulated through the choice of substrate temperature. The most photostable PVD glass is 50 times more resistant to light irradiation than the liquid-cooled glass. We observe that photostability is highly correlated with the density of the vapor-deposited glasses. Molecular simulations of photoisomerization in vapor-deposited glasses are able to capture the key features observed in the experiments and provide further molecular-level insight into the mechanism of stability. In particular, the tight molecular packing of the denser glass creates higher energy barriers for molecular rearrangement, which then inhibits the photoisomerization reaction. We expect that enhanced photostability is a general property of dense vapor-deposited glasses that may also be exploited with other molecular systems including those used in organic electronics.

2. RESULTS AND DISCUSSION

2.1. Vapor-Deposited DO37 Forms Glasses with High Kinetic Stability. As an initial step in these experiments, we used spectroscopic ellipsometry to characterize the kinetic stability and density of PVD glasses of DO37. Figure 1 shows an example of a temperature-ramping experiment for a DO37 glass vapor-deposited at $T_{substrate}$ = 260 K (0.88T_g). Three different ramping cycles were performed. In the first cycle, the as-deposited sample was first heated from 288 to 320 K and then cooled to 288 K. Subsequent heating and cooling cycles between 288 and 310 K are also shown, and all heating/cooling rates were 1 K/min. During the first cycle of heating, the initial increase in thickness (below 303 K) is due to thermal expansion of the as-deposited glass. At the onset temperature (T_{onset}), the as-deposited glass begins to transform into a supercooled liquid. During subsequent cooling, the supercooled liquid falls out of equilibrium and transforms into a glass at T_g. As expected, the second and third cooling runs shown in Figure 1 are indistinguishable from the first cooling because they all started in the equilibrium supercooled liquid.

The as-deposited glass of DO37 in Figure 1 shows high kinetic stability and high density relative to the liquid-cooled glass. The high T_{onset} (12 K above T_g) required to transform the as-deposited glass into the supercooled liquid is an indication of enhanced kinetic stability. The change in thickness between the first heating and cooling cycles is used to determine the density of the as-deposited glass relative to the liquid-cooled glass ($\Delta\rho$). In this case, the as-deposited glass is 1.3% more dense,

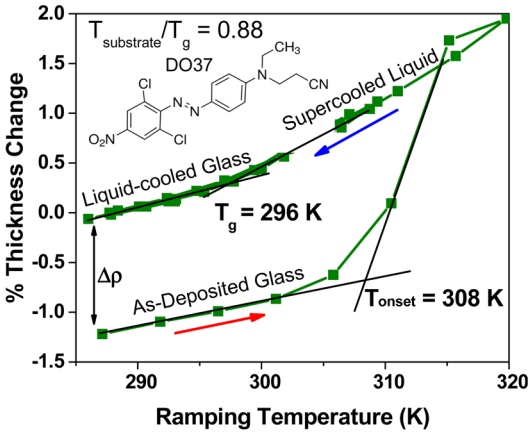

Figure 1. Thickness changes for a vapor-deposited glass of DO37 during temperature ramping at 1 K/min. The green symbols represent experimental data for a sample prepared at $T_{substrate}$ = 0.88T_g. Black lines are linear extrapolations that demonstrate the determination of T_g (for the liquid-cooled glass) and the onset temperature T_{onset} (for the as-deposited glass). $\Delta\rho$ shows the density difference between the as-deposited and liquid-cooled glass. The inset shows the molecular structure of DO37.

consistent with more efficient local packing and higher kinetic stability. Vapor-deposited glasses of DO37 have properties similar to those of other PVD glasses with high kinetic stability.[15,16,18,19,25−28] For comparison, indomethacin, an extensively studied system, has been reported to form glasses with T_{onset} as high as 18 K above T_g, along with density increases of up to 1.4%.[21]

The kinetic stability of vapor-deposited DO37 glasses depends on the choice of substrate temperature during PVD. As indicated by the inset in Figure 2, DO37 glasses were

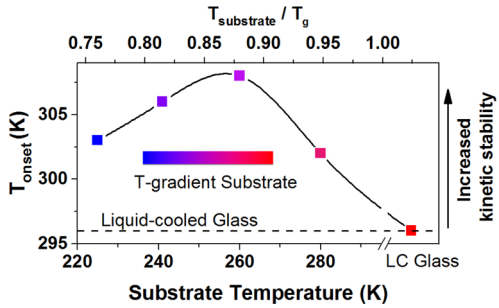

Figure 2. Kinetic stability of DO37 glasses vapor-deposited at different substrate temperatures. T_{onset} represents the onset of glass transformation during heating of 1 K/min. All glasses were prepared during one deposition on a temperature gradient substrate. The inset schematically indicates a temperature-gradient across the substrate. The solid black line is a guide to the eye.

prepared on a substrate that had an imposed temperature gradient ranging from 0.75 T_g to above T_g. In this way, a library of glasses was prepared in one deposition. The detailed method of sample preparation is presented in the Methods section. For glasses deposited above T_g (296 K), the as-deposited sample had the same onset temperature as the liquid-cooled (LC) glass. For $T_{substrate}$ lower than T_g, enhanced kinetic stability was obtained. The optimal $T_{substrate}$ for kinetic stability is 0.88T_g (Figure 2), which is similar to indomethacin and other molecular systems.[22] The increased kinetic stability and density of vapor-deposited films is attributed to enhanced surface

DOI: 10.1021/jacs.6b06372
J. Am. Chem. Soc. 2016, 138, 11282−11289

mobility during film formation.[24,29−31] Freshly deposited molecules have enough mobility to efficiently sample packing arrangements, resulting in near-equilibrium local packing well below T_g; subsequent deposition locks this efficient packing into the glassy film. The optimal stability obtained by deposition onto substrates near $0.88T_g$ is a result of the competition between kinetic and thermodynamic control.[22] At lower temperatures, surface mobility is not high enough to allow access to better packing arrangements even though the thermodynamic driving force is larger.

2.2. PVD Glasses Exhibit Enhanced Photostability. The photostability of DO37 glasses was monitored by spectroscopic ellipsometry during light irradiation. Density and birefringence, representing molecular packing and molecular orientation, respectively, can be obtained by ellipsometry and were used to characterize photostability of the glassy thin films. As shown in Scheme 1, a 532 nm laser was used to irradiate the thin glass samples and induce photoisomerization. Simultaneously, spectroscopic ellipsometry measured the thickness and birefringence changes in the irradiated area. The in-plane sample dimensions are fixed, so density is inversely related to thickness.

Scheme 1. Experimental Test of Photostability for Glassy Thin Films[a]

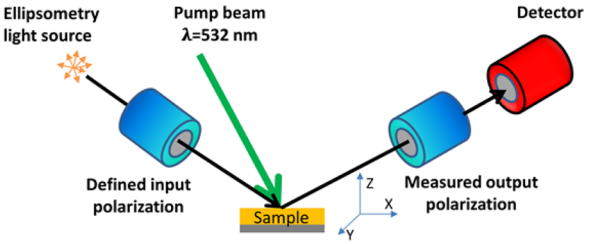

[a]A 532 nm laser is used to irradiate the DO37 thin film inducing photoisomerization. Simultaneously, spectroscopic ellipsometry is used to measure thickness and birefringence changes in the film.

A comparison of the light-induced density and birefringence changes for PVD and liquid-cooled glasses, as shown in Figure 3, reveals that the PVD glasses display significantly enhanced photostability. The density of the liquid-cooled glass decreases immediately after irradiation begins and reaches steady-state in tens of seconds. In contrast, PVD glasses can maintain their original density for hundreds to thousands of seconds, depending on the substrate temperature at which the sample was deposited. The birefringence measurements also show that vapor-deposited glasses are more photostable; molecules in PVD glasses are more resistant to light-driven changes in molecular orientation. Both *s*- and *p*-polarized irradiation result in similar trends. Results for *s*-polarized irradiation are shown in Figure 3, while results for *p*-polarized irradiation are given in Figure S1.

Previous studies of azobenzene-containing glasses under irradiation have proposed mechanisms that qualitatively explain the density and birefringence changes shown in Figure 3.[32−35] Trans → cis → trans cycling disrupts packing in the glassy matrix due to changes in molecular shape and molecular volume.[36,37] Because of the very long relaxation time of the glass, molecules have little opportunity to reoptimize their local packing during irradiation, and thus density decreases. Changes in birefringence during irradiation can be attributed to the photoalignment effect.[34] When a molecule returns to the trans

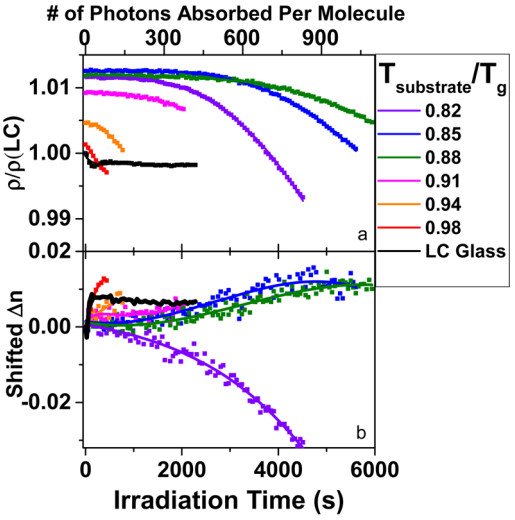

Figure 3. Density and birefringence changes for vapor-deposited and liquid-cooled glasses of DO37 as a function of irradiation time. (a) Glass density relative to initial density of the liquid-cooled glass. (b) Birefringence Δn relative to as-deposited glass. Lines are guides to the eye.

state after isomerization, it need not have the same orientation as it had initially. Repeated photoisomerization with polarized light has the net effect of increasing the fraction of molecules whose transition dipoles are orthogonal to the excitation polarization because these molecules do not have the opportunity for further photoisomerization; the sample thus becomes anisotropic and birefringent. We note that most as-deposited glasses of DO37 showed negative initial birefringence (Figure S2). In Figure 3b, the birefringence is shifted so that the initial value is zero for all glasses for easier comparison.

2.3. Photostability Correlates with Glass Density. To quantitatively compare photostability of vapor-deposited and liquid-cooled glasses, we further analyze the experimental results presented above. Figure 4a shows the irradiation times required to achieve small changes in density and birefringence. These small changes in density (0.1%) and birefringence (0.005) represent the initial structural alteration of the glasses, at a stage where the glasses have not yet lost their initial material properties. Photostabilities deduced from these two observables are highly consistent. For comparison, Figure 4b shows the density for DO37 glasses vapor-deposited at different substrate temperatures relative to the liquid-cooled glass. All glasses deposited with $T_{substrate} < T_g$ show higher densities than the liquid-cooled glass. The maximum density is observed for a substrate temperature of 0.86 T_g, which is consistent with previously reported results for vapor-deposited glasses of indomethacin.[21]

By comparing Figure 4a,b, it is evident that there is a strong correlation between photostability and glass density and that the higher density of the PVD glasses is associated with a 50-fold increase in photostability. As we discuss further below, there is no precedent for such a large effect of glass packing at ambient pressure. In a study of an azobenzene derivative tethered to a PMMA polymer, it was demonstrated that optically induced molecular orientation can be hindered by density increases caused by high pressure[38] compared to ambient pressure, where the glass density at 150 MPa was increased by 2.4% and the rate of photo-orientation decreased by a factor of nearly 50. This high-pressure work demonstrated

DOI: 10.1021/jacs.6b06372
J. Am. Chem. Soc. 2016, 138, 11282−11289

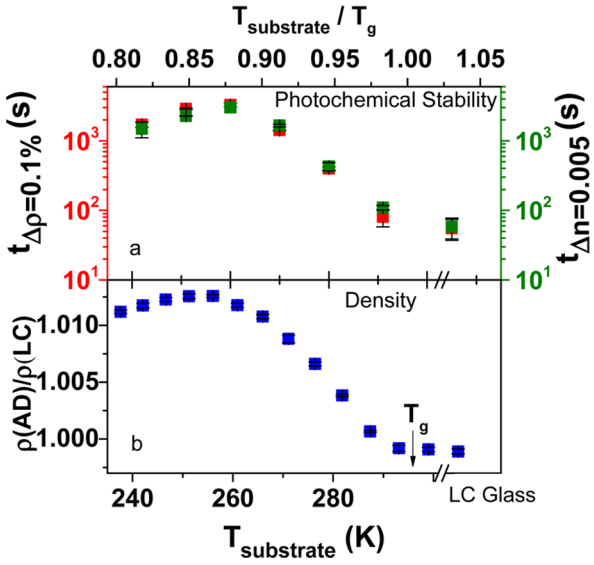

Figure 4. Photostability and density of PVD glasses of DO37, with comparison to the liquid-cooled (LC) glass. A strong correlation is observed between photostability and density. (a) Irradiation time required to achieve a 0.1% density change (red) and 0.005 birefringence change (green). (b) Density of as-deposited (AD) glasses relative to the LC glass. For substrate temperature below T_g, vapor-deposited glasses show increased density, and the maximum density occurs at 255 K (0.86 T_g).

a correlation between density and photostability that is qualitatively consistent with the results in Figure 4. However, in the work of ref 38, enhanced photostability was only observed at high pressure, and the rate of photoisomerization became fast again when the pressure was released. In contrast, the present work provides a method to increase the photostability of ambient-pressure materials.

To test the generality of the effect of enhanced photostability, we performed additional experiments at a lower irradiation temperature and found that PVD glasses of DO37 become even more photostable relative to the liquid-cooled glass. In the field of organic electronics, materials are usually used at temperatures at least 30−40 K below T_g. In contrast, for experiments described in Figures 3 and 4, the measurement temperature was 287 K, only 9 K below the T_g for DO37. For a few experiments, we lowered the measurement temperature to 278 K (T_g − 18 K) to get closer to the conditions for many applications. For PVD glasses, the photostability results are nearly the same at 278 and 287 K (Figure S4). For the liquid-cooled glass, however, photoinduced density and birefringence changes occurred more quickly at lower temperature (Figure S5), such that the PVD glasses are even more photostable at lower temperature, relative to the liquid-cooled glass. This behavior of the liquid-cooled glass can be attributed to the competition between photoinduced changes and structural relaxation back toward equilibrium.[39] At lower temperatures, structural relaxation becomes slower, allowing illumination to more quickly drive the system away from equilibrium.

2.4. Molecular Simulations of PVD Glasses. Molecular simulations of the vapor deposition and photoisomerization processes were performed to understand the mechanism of enhanced photostability in PVD glasses. To focus on the key physics responsible for the packing effects observed in our experiments, we propose a simple model to examine isomerization, namely, a linearly connected molecule of four beads that serves as a coarse-grained representation of DO37 (Figure 5, inset). During the vapor deposition portion of the

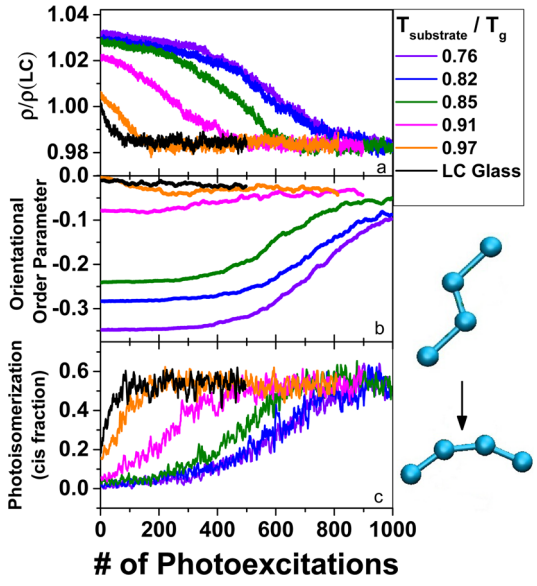

Figure 5. Simulations of photostability for vapor-deposited and liquid-cooled (LC) glasses as a function of photoexcitation cycle. (a) Glass density relative to LC glass (ρ/ρ(LC)). (b) Orientation order parameter. (c) Fraction of successful trans → cis conversions in each photoexcitation. Representative structures of the coarse-grained model in trans and cis states are shown on the right panel.

simulations, which utilized a procedure employed in previous simulations of PVD glasses,[23,24,40,41] these molecules were held in the trans state. Glass films were deposited onto substrates at temperatures ranging from 0.76T_g to 0.97T_g, where T_g was determined to be 0.66 (in reduced Lennard-Jones (LJ) units) by simulations in which the liquid was cooled into the glass. (Figure S6). Consistent with the experimental results in Figure 4b, all the simulated PVD glasses had higher density than the liquid-cooled glass (Table S1). During the photoisomerization portion of the simulations, an iterative method mimicking the stochastic process of photoexcitation described in the Methods section was used to test the photostability of each of the glasses formed. In brief, a few molecules are "photoexcited" by instantaneously switching the dihedral potential from the initial state (where trans is the stable state) to a new potential (where cis is the stable state). Molecular dynamics simulations are then continued with the local packing environment of each molecule determining whether or not the cis state can actually be reached. After a period of time (mimicking the excited state lifetime), the potential is switched back to the original one favoring the trans state. This process is repeated many times where molecules are selected at random for photoexcitation.

Figure 5 shows that the simulated PVD glasses have substantially increased photostability relative to the liquid-cooled glass, in qualitative agreement with the experimental results shown in Figure 3. The top panel of Figure 5 shows that the PVD glasses which have higher initial densities than the liquid-cooled glass maintain their initial density for a greater number of photoexcitation cycles. The middle panel of Figure 5 shows the orientation order parameter, S_z, of the simulated glasses as a function of the number of photoexcitation steps; S_z represents the average orientation of transition dipoles for simulated molecules and can be qualitatively compared with the

DOI: 10.1021/jacs.6b06372
J. Am. Chem. Soc. 2016, 138, 11282−11289

experimentally measured birefringence. Although only small changes in orientation occur for the liquid-cooled glass, they occur much more quickly than for the PVD glasses. Figure S3 quantifies photostability using these results and shows that the simulated PVD glasses are at least 10 times more photostable than the liquid-cooled glass. In addition, the simulation results display a strong correlation between photostability and glass density, in agreement with experiment (Figure S3).

The simulation trajectories indicate that the initial molecular packing of higher density glasses restricts excited molecules from reaching the cis state, even though their molecular potential strongly favors the cis state. The fraction of successful isomerization events is shown as a function of photoexcitation cycles for each glass in Figure 5c. This is loosely equivalent to the quantum yield for the actual photoisomerization reaction. For the highest density glasses, there is a very low probability for a successful isomerization event, and this explains the very slow initial changes in the density and S_z parameter.

2.5. Mechanism for Enhanced Photostability. We considered two possible mechanisms for the enhanced photostability of high-density PVD glasses shown in Figures 3 and 4. According to one possible mechanism, photoisomerization to the cis state occurs only rarely in the highest density PVD glasses (due to efficient packing) but occurs much more frequently in lower density glasses. For the second possible mechanism, we imagine that photoisomerization to the cis state occurs efficiently in all glasses, but that only the low density glasses are restructured as a result. We favor the first mechanism, and our simulation results strongly support this view. Figure 5c shows that for the highest density vapor-deposited glasses the isomerization from trans to cis is nearly completely prevented in the simulations. In the simulation, photoexcitation provides an intramolecular driving force to leave the trans state, but in high density glasses, most molecules are unable to reconfigure due to efficient packing. For lower density glasses, the intermolecular barrier for rearrangement will be lower, allowing molecules to achieve the cis state with higher probability.

We performed additional experiments to directly test the hypothesis that molecules in a dense glass rarely reach the cis state as a result of photoexcitation. DO37 is a "push−pull" azobenzene, and consistent with other azobenzene derivatives of this type, the lifetime of the cis state for DO37 is reported to be less than 1 s.[42] Our efforts to directly detect depletion of the trans state in the absorption spectrum during irradiation were unsuccessful, even for the liquid-cooled glass. A reasonable interpretation of these results is that the steady-state population of the cis state in our experiments is always quite low. While we expect that the cis state population during irradiation is lower for denser glasses than for the liquid-cooled glass, we have not directly established this.

Our proposed mechanism is consistent with literature evidence that the local packing environment can influence the ability of photoexcited azobenzenes to reach the cis state. For example, in a glass of 4,4′-diphenyl azobenzene dispersed in amorphous polycarbonate, it was shown that physical aging for 100 h caused an ∼5% decrease in the photoisomerization quantum yield relative to the glass prepared by liquid cooling;[14] because a symmetric azobenzene with a long cis lifetime was used in this study, this result could be seen directly as depletion of trans state absorption. Aging for 100 h likely increases density by much less than 1.3%, and this provides a way to understand the much larger effects on photostability obtained in our study with PVD glasses. In another study, azobenzene derivatives were incorporated into different DNA sequences so that the local packing could be tuned by changing the neighboring base pairs.[43] In this system, it was demonstrated that the quantum yield of azobenzene photoisomerization decreased with increased restriction of molecular packing, varying by a factor of 4. Additionally, the photoisomerization of crystalline *trans*-azobenzene is severely hindered in the bulk crystal.[44] These studies all support the idea that the quantum yield for photoisomerization to the cis state decreases with increasing intermolecular barriers for molecular rearrangement.

Considering that literature precedents and our simulations both support the view that denser glasses can prevent photoisomerization, it is useful to estimate the magnitude of the intermolecular barriers for rearrangement in PVD and liquid-cooled glasses. Figure 6 shows the energy diagram for

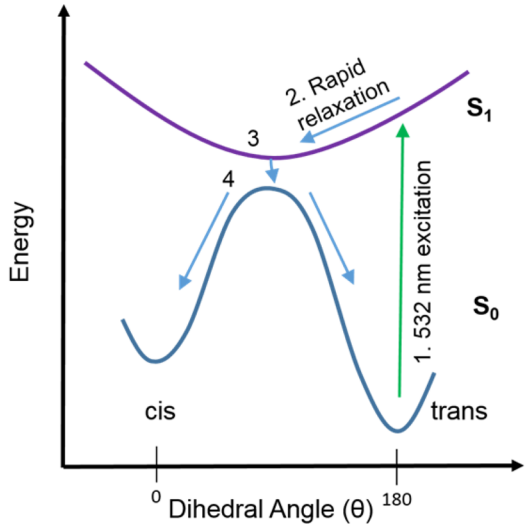

Figure 6. Energy diagram of photoisomerization for DO37.

photoisomerization of an azobenzene in the gas phase and provides background for our discussion. After a 532 nm photon causes excitation to the S_1 state, the molecule relaxes to a twisted configuration ($\theta = 90°$). Upon transition to the ground state, the molecule either twists forward to the cis state or back to the trans state with roughly equal probability.[45] In a glass, for an azobenzene molecule to transition from trans to cis, it must additionally overcome intermolecular barriers in an environment that is quite rigid and essentially static on the time scale of photoexcitation. Using measurements and estimates of the structural relaxation times, we can estimate the activation free energies for cooperative rearrangements in the liquid-cooled and PVD glasses to be 34 and 51 kT, respectively (see Supporting Information). We now imagine adding an intermolecular potential favoring the trans state to the diagram in Figure 6. The barrier for rearrangement in the high density glass is a large fraction of the photon energy (94 kT at the experimental temperature), so it is plausible that the intermolecular packing blocks any significant progress toward the cis state in the dense glass while this mechanism would be less efficient in the liquid-cooled glass. A weakness of this argument is that we have no experimental estimate of the intermolecular barrier associated with photoisomerization, but given the size of the molecular rearrangement required to reach the cis state, it is reasonable that it will be not too much smaller

DOI: 10.1021/jacs.6b06372
J. Am. Chem. Soc. 2016, 138, 11282−11289

than the barrier for structural relaxation. A more detailed theoretical study will be required to examine our proposed mechanism more rigorously.

3. CONCLUSIONS

In this study, we have established that vapor-deposited organic glasses can be much more photostable than liquid-cooled glasses. While previous work on crystals indicated the important influence of local packing, this is the first demonstration of a significant impact of different amorphous packing arrangements on the photostability of organic molecules. We showed that high-density glasses of DO37 can be made by PVD and that the density can be systematically varied through controlling the substrate temperature. The highest density glass was 50 times more photostable than the liquid-cooled glass, and we find a strong correlation between photostability and glass density. We attribute this effect to the high intermolecular barriers for rearrangement that are present in the highest density PVD glasses. This view is supported by molecular simulations of coarse-grained DO37 molecules that successfully reproduced the high density and high photostability of the PVD glasses. The simulations show that in the highest density glasses the local packing environment prevents photoexcited molecules from escaping the trans configuration.

We expect that enhancement in photostability for vapor-deposited glasses is a general effect that will be observed for many molecular systems beyond the azobenzenes. To date, PVD has prepared glasses with high kinetic stability from more than 30 organic molecules, including several molecules used in the active layers of organic light-emitting diodes (OLEDs).[20] In every case where it has been checked, glasses with high kinetic stability also have high density relative to the liquid-cooled glass. Thus, we expect that PVD glasses of many organic molecules will show an increased energy barrier for molecular rearrangements that will slow photoreactions. This may be particularly useful in applications where photodegradation leads to deterioration of performance, as in OLEDs and organic photovoltaics. For example, operational lifetime is considered to be a bottleneck to the further improvement of OLED display performance, especially for blue emitters.[46] It has been found that degradation of OLEDs can be caused by self-luminescence,[9] electrochemical reaction,[47] and hole injection.[48] We speculate that high-density PVD glasses might delay degradation of OLED molecules as a result of any of these processes because our results indicate that efficient packing can inhibit chemical processes. OLEDs are already produced by PVD, so optimizing the substrate temperature to produce the densest glass might thus increase device lifetime. We do not expect that all organic glasses will show a 2 orders of magnitude enhancement in photostability as a result of optimal vapor deposition. Azobenzenes require a particularly large rearrangement for photoisomerization, and it is likely that photodegradation processes that require smaller rearrangements will be less impacted by the local packing. Future work should investigate the impact of glass packing on a range of different chemical and photochemical processes.

4. EXPERIMENT AND SIMULATION METHODS

4.1. Materials. Disperse Orange 37 (DO37, 99% purity) was obtained from Santa Cruz Biotechnology and used as received. DO37 was selected for these experiments because it has a T_g higher than room temperature; it is a reasonably good glass former, which facilitates glassy thin film preparation via the PVD process. Differential scanning calorimetry (DSC) measurements show that the glass transition temperature (T_g) for DO37 is 296 K, with a 10 K/min cooling and heating rate, which is in good agreement with ellipsometry results. Prior to performing the DSC measurements, the material was first melted, then quenched in liquid nitrogen.

4.2. Physical Vapor Deposition. PVD was performed in a vacuum chamber with a base pressure of 10^{-7} Torr. Crystalline DO37 was placed in a crucible that was resistively heated. The deposition rate was controlled by tuning the heater power and monitored by a quartz crystal microbalance (QCM). The deposition rate was kept at a constant value of 2 Å/s for all experiments. The final sample thicknesses were about 300 nm. A high throughput method was utilized to prepare a library of glasses with different densities and kinetic stabilities.[21] The substrate (Si wafer) was suspended between two copper fingers; different temperatures were imposed at each finger to create a temperature gradient across the sample during deposition. The substrate temperature range was from 240 to 305 K.

4.3. Kinetic Stability and Density Measurements. Kinetic stability and density of vapor-deposited thin films were characterized by spectroscopic ellipsometry, an optical technique that measures thickness and refractive indices of thin films. For all ellipsometry measurements, three incident angles were used (50, 60, and 70°), and wavelengths from 370 to 1000 nm were utilized. To measure kinetic stability, ellipsometry was performed on samples placed on a custom-built hot stage, and the temperature was increased at 1 K/min from near room temperature to 25 K above T_g. The onset temperature, which characterizes the kinetic stability of a glass, was determined from the beginning of the transformation into the supercooled liquid, as shown in Figure 1. Immediately after heating, the supercooled liquid was cooled at 1 K/min into the liquid-cooled glass. By comparing sample thickness before and after temperature cycling, the density of the vapor-deposited glass relative to the liquid-cooled glass can be determined.

4.4. Photostability Measurement. The light irradiation experiment used to test photostability of PVD glasses is shown in Scheme 1. A linearly polarized 532 nm laser was used as the light source to induce the photoisomerization reaction at a power level of 11 mW/cm^2. During irradiation, spectroscopic ellipsometry was used to characterize the glass thickness and birefringence at the same spot where the 532 nm laser irradiated the sample. In this way, photoinduced structural changes of the thin glassy films were monitored in real time. The photostability tests shown in the main text were performed at 287 K (T_g − 9 K). To model the ellipsometric data observed during light irradiation, a biaxial anisotropic Cauchy model was used. This model allows three independent refractive indices, which is necessary because irradiation generates anisotropy in the glass sample along a different axis than the anisotropy generated in the deposition process. In the measurement of photostability, birefringence is defined as the refractive index difference $n_z - n_x$ at 980 nm, where n_z and n_x represent refractive indices for light polarized along the substrate normal and the x direction in the plane of the substrate, respectively; see Scheme 1 for coordinate system.

4.5. Computer Simulations. Molecular dynamics simulations of a coarse-grained model of DO37 were performed to study photoisomerization of vapor-deposited glasses at a molecular level. The model consists of four linearly connected LJ particles (Figure 5) with parameters σ_{bb} = 1.0 and ε_{bb} = 1.0. (All units reported for the simulations are reduced LJ units.) The cutoff distance for the potential is r_c = 2.5 with a smooth decay starting at r = 2.4. To mimic the structure of azobenzene, the four particles were held together by three stiff harmonic bonds with the inner bond shorter than the two outer bonds (l_{inner} = 1.0, l_{outer} = 1.5, and k_b = 1000). The two bond angles were controlled by a harmonic potential with values that mimic sp^2 hybridization (θ = 120°; k_{angle} = 1000). As described below, the dihedral angle potential was switched in order to mimic the photoexcitation process. The dihedral angles for the trans and cis potentials were defined by

$$U_{dihedral} = \frac{1}{2}k_1(1 + \cos\theta) + \frac{1}{2}k_2(1 - \cos 2\theta)$$

DOI: 10.1021/jacs.6b06372
J. Am. Chem. Soc. 2016, 138, 11282−11289

where $k_1 = 20$ and $k_2 = 8$ for the trans state and $k_1 = -25$ and $k_2 = 6.25$ for the cis state.

Vapor-deposited glasses were generated in a simulation box with dimensions of $20\sigma_{bb}$ by $20\sigma_{bb}$ in the plane of the substrate (xy-plane), and at least $10\sigma_{bb}$ larger than the deposited film thickness in the normal direction to the substrate (z-dimension). Periodic boundary conditions were applied to the x- and y-dimensions. The substrate was generated from 1000 randomly placed smaller particles. The potential parameters for the substrate are chosen to minimize any ordering effect on the deposited material while still being able to anchor the growing film.[40] The interaction parameters for substrate atoms are $\sigma_{ss} = 0.6$ and $\varepsilon_{ss} = 0.1$, and the interaction parameters for the deposited molecules with the substrate are $\sigma_{sb} = 0.75$ and $\varepsilon_{sb} = 1.0$, with a cutoff distance of $2.5\sigma_{\alpha\beta}$, where $\alpha,\beta \in$ (s,b). The substrate atoms are fixed to their initial position by harmonic springs. The simulated vapor deposition process is analogous to that reported earlier.[23,24,40,41] At least 850 deposition steps were performed for each glass film in order to achieve a film thickness of at least $40\sigma_{bb}$. The middle section of the film ($15\sigma_{bb}$ to $28\sigma_{bb}$ in the z-dimension) was used to calculate bulk glass properties to avoid the influence of the substrate or the free surface. The deposition cycle consists of four repeated steps: (i) introduction of four randomly oriented molecules above but in close proximity to the film surface, (ii) equilibration of the newly introduced molecules at high temperature ($T = 1.25$), (iii) linear cooling over 2000 time units of these molecules to the substrate temperature, and finally, (iv) minimization of the energy for the entire system. A separate thermostat is used to maintain the previously deposited molecules and substrate particles at the desired substrate temperature throughout the cycle. For the entire film preparation process described above, the trans dihedral potential was utilized. All simulations were performed using the Large-Scale Atomic/Molecular Massively Parallel Simulator (LAMMPS) package[49] in the canonical ensemble with a simulation time step of 0.001 LJ time units. The orientation order parameter, S_z, was used to characterize the average orientation of the simulated films. S_z is defined as

$$S_z = \frac{3}{2} < \cos^2 \delta_z > -1$$

where δ_z is the angle of the molecular end-to-end vector relative to the substrate normal.

An iterative process was used to simulate the photoisomerization reaction. To mimic photoexcitation, a small group of selected molecules have their dihedral angle potential temporarily switched from trans to cis. During the short molecular dynamics trajectory that follows (mimicking the excited state lifetime), these selected molecules may transition to the cis state or their environment may trap them with a dihedral angle close to the trans state, i.e., although their dihedral angle potentials were changed to favor the cis state, the selected molecules were not forced to the cis state. To avoid influences from the interfaces, only the bulk region of the simulated film was considered for the photoisomerization process. To capture the directionality of the polarized light, a director vector was used as a proxy, which pointed 30° off the substrate normal. All photoexcitation simulations were carried out at $T = 0.6$ ($0.9\ T_g$). Each cycle included the following steps: (1) select a molecule at random, (2) accept or reject for excitation with probability $\cos^2(\gamma)$, where γ is the angle between the director vector and the end-to-end vector of the molecule, (3) continue first two steps until 1% of the bulk molecules have been accepted, (4) switch the dihedral potential for the selected molecules from trans to cis, (5) run molecular dynamics for 100 time units, and (6) return all dihedral potentials to the trans potential.

■ ASSOCIATED CONTENT

Supporting Information

The Supporting Information is available free of charge on the ACS Publications website at DOI: 10.1021/jacs.6b06372.

Additional data (polarized light measurements, initial birefringence as a function of substrate temperature, correlation of photostability with glass density, photostability as a function of irradiation time, intensive potential energy calculated for the bulk region of the film, and comparison of glasses of the DO37 system) and discussions (PDF)

■ AUTHOR INFORMATION

Corresponding Author

*ediger@chem.wisc.edu

Funding

NSF DMR-1234320 and DE-SC0002161.

Notes

The authors declare no competing financial interest.

■ ACKNOWLEDGMENTS

We thank Trisha Andrew, Robert McMahon, and Lian Yu for helpful discussions, and Men Zhu for help with DSC experiments. In addition, M.D.E. acknowledges a conversation with the late Paul Barbara that stimulated these experiments. The experimental work was supported by the U.S. Department of Energy, Office of Basic Energy Sciences, Division of Materials Sciences and Engineering, Award DE-SC0002161 (to M.D.E. and Y.Q.). The simulations were supported by NSF DMR-1234320 (to J.J.dP. and L.W.A.).

■ REFERENCES

(1) Soutis, C. *Mater. Sci. Eng., A* **2005**, *412*, 171.
(2) Yu, L. *Adv. Drug Delivery Rev.* **2001**, *48*, 27.
(3) Chen, Y. H.; Lin, L. Y.; Lu, C. W.; Lin, F.; Huang, Z. Y.; Lin, H. W.; Wang, P. H.; Liu, Y. H.; Wong, K. T.; Wen, J. G.; Miller, D. J.; Darling, S. B. *J. Am. Chem. Soc.* **2012**, *134*, 13616.
(4) Yokoyama, D. *J. Mater. Chem.* **2011**, *21*, 19187.
(5) Shirota, Y.; Kageyama, H. *Chem. Rev.* **2007**, *107*, 953.
(6) Hancock, B. C.; Parks, M. *Pharm. Res.* **2000**, *17*, 397.
(7) Kushida, I.; Ichikawa, M.; Asakawa, N. *J. Pharm. Sci.* **2002**, *91*, 258.
(8) Holmes, R. J.; Forrest, S. R.; Tung, Y. J.; Kwong, R. C.; Brown, J. J.; Garon, S.; Thompson, M. E. *Appl. Phys. Lett.* **2003**, *82*, 2422.
(9) Wang, Q.; Luo, Y. C.; Aziz, H. *Appl. Phys. Lett.* **2010**, *97*, 063309.
(10) Seifert, R.; Rabelo de Moraes, I. R.; Scholz, S.; Gather, M. C.; Lussem, B.; Leo, K. *Org. Electron.* **2013**, *14*, 115.
(11) Rezzonico, D.; Jazbinsek, M.; Gunter, P.; Bosshard, C.; Bale, D. H.; Liao, Y.; Dalton, L. R.; Reid, P. J. *J. Opt. Soc. Am. B* **2007**, *24*, 2199.
(12) Schmidt, G. M. J. *Pure Appl. Chem.* **1971**, *27*, 647.
(13) Cohen, M. D.; Schmidt, G. M. J. *J. Chem. Soc.* **1964**, 1996.
(14) Royal, J. S.; Torkelson, J. M. *Macromolecules* **1992**, *25*, 4792.
(15) Swallen, S. F.; Kearns, K. L.; Mapes, M. K.; Kim, Y. S.; McMahon, R. J.; Ediger, M. D.; Wu, T.; Yu, L.; Satija, S. *Science* **2007**, *315*, 353.
(16) Leon-Gutierrez, E.; Garcia, G.; Clavaguera-Mora, M. T.; Rodriguez-Viejo, J. *Thermochim. Acta* **2009**, *492*, 51.
(17) Sepulveda, A.; Tylinski, M.; Guiseppi-Elie, A.; Richert, R.; Ediger, M. D. *Phys. Rev. Lett.* **2014**, *113*, 045901.
(18) Rodriguez-Tinoco, C.; Gonzalez-Silveira, M.; Rafols-Ribe, J.; Garcia, G.; Rodriguez-Viejo, J. *J. Non-Cryst. Solids* **2015**, *407*, 256.
(19) Ramos, S. L. M.; Chigira, A. K.; Oguni, M. *J. Phys. Chem. B* **2015**, *119*, 4076.
(20) Dalal, S. S.; Walters, D. M.; Lyubimov, I.; de Pablo, J. J.; Ediger, M. D. *Proc. Natl. Acad. Sci. U. S. A.* **2015**, *112*, 4227.
(21) Dalal, S. S.; Fakhraai, Z.; Ediger, M. D. *J. Phys. Chem. B* **2013**, *117*, 15415.
(22) Kearns, K. L.; Swallen, S. F.; Ediger, M. D.; Wu, T.; Sun, Y.; Yu, L. *J. Phys. Chem. B* **2008**, *112*, 4934.
(23) Lyubimov, I.; Antony, L.; Walters, D. M.; Rodney, D.; Ediger, M. D.; de Pablo, J. J. *J. Chem. Phys.* **2015**, *143*, 094502.

DOI: 10.1021/jacs.6b06372
J. Am. Chem. Soc. 2016, 138, 11282−11289

(24) Lyubimov, I.; Ediger, M. D.; de Pablo, J. J. *J. Chem. Phys.* **2013**, *139*, 144505.
(25) Tylinski, M.; Sepulveda, A.; Walters, D. M.; Chua, Y. Z.; Schick, C.; Ediger, M. D. *J. Chem. Phys.* **2015**, *143*, 244509.
(26) Zhu, L.; Yu, L. A. *Chem. Phys. Lett.* **2010**, *499*, 62.
(27) Dawson, K.; Zhu, L.; Kopff, L. A.; McMahon, R. J.; Yu, L.; Ediger, M. D. *J. Phys. Chem. Lett.* **2011**, *2*, 2683.
(28) Walters, D. M.; Richert, R.; Ediger, M. D. *J. Chem. Phys.* **2015**, *142*, 134504.
(29) Zhu, L.; Brian, C. W.; Swallen, S. F.; Straus, P. T.; Ediger, M. D.; Yu, L. *Phys. Rev. Lett.* **2011**, *106*, 4.
(30) Zhang, W.; Brian, C. W.; Yu, L. *J. Phys. Chem. B* **2015**, *119*, 5071.
(31) Stevenson, J. D.; Walczak, A. M.; Hall, R. W.; Wolynes, P. G. *J. Chem. Phys.* **2008**, *129*, 194505.
(32) Tanchak, O. M.; Barrett, C. J. *Macromolecules* **2005**, *38*, 10566.
(33) Hagen, R.; Bieringer, T. *Adv. Mater.* **2001**, *13*, 1805.
(34) Sekkat, Z.; Wood, J.; Knoll, W. *J. Phys. Chem.* **1995**, *99*, 17226.
(35) Bennani, O. R.; Al-Hujran, T. A.; Nunzi, J. M.; Sabat, R. G.; Lebel, O. *New J. Chem.* **2015**, *39*, 9162.
(36) Harada, J.; Ogawa, K. *J. Am. Chem. Soc.* **2004**, *126*, 3539.
(37) Mostad, A.; Rømming, C. *Acta Chem. Scand.* **1971**, *25*, 3561.
(38) Sekkat, Z.; Kleideiter, G.; Knoll, T. *J. Opt. Soc. Am. B* **2001**, *18*, 1854.
(39) Tanino, T.; Yoshikawa, S.; Ujike, T.; Nagahama, D.; Moriwaki, K.; Takahashi, T.; Kotani, Y.; Nakano, H.; Shirota, Y. *J. Mater. Chem.* **2007**, *17*, 4953.
(40) Singh, S.; Ediger, M. D.; de Pablo, J. J. *Nat. Mater.* **2013**, *12*, 139.
(41) Lin, P. H.; Lyubimov, I.; Yu, L.; Ediger, M. D.; de Pablo, J. J. *J. Chem. Phys.* **2014**, *140*, 204504.
(42) Dokic, J.; Gothe, M.; Wirth, J.; Peters, M. V.; Schwarz, J.; Hecht, S.; Saalfrank, P. *J. Phys. Chem. A* **2009**, *113*, 6763.
(43) Yan, Y. Q.; Wang, X.; Chen, J. I. L.; Ginger, D. S. *J. Am. Chem. Soc.* **2013**, *135*, 8382.
(44) Nakayama, K.; Jiang, L.; Iyoda, T.; Hashimoto, K.; Fujishima, A. *Jpn. J. Appl. Phys. 1* **1997**, *36*, 3898.
(45) Crecca, C. R.; Roitberg, A. E. *J. Phys. Chem. A* **2006**, *110*, 8188.
(46) Zhang, Y. F.; Lee, J.; Forrest, S. R. *Nat. Commun.* **2014**, *5*, 5008.
(47) Papadimitrakopoulos, F.; Zhang, X.-M.; Higginson, K. A. *IEEE J. Sel. Top. Quantum Electron.* **1998**, *4*, 49.
(48) Aziz, H.; Popovic, Z. D.; Hu, N. X.; Hor, A. M.; Xu, G. *Science* **1999**, *283*, 1900.
(49) Plimpton, S. *J. Comput. Phys.* **1995**, *117*, 1.

DOI: 10.1021/jacs.6b06372
J. Am. Chem. Soc. 2016, 138, 11282−11289